

Supplementary Materials

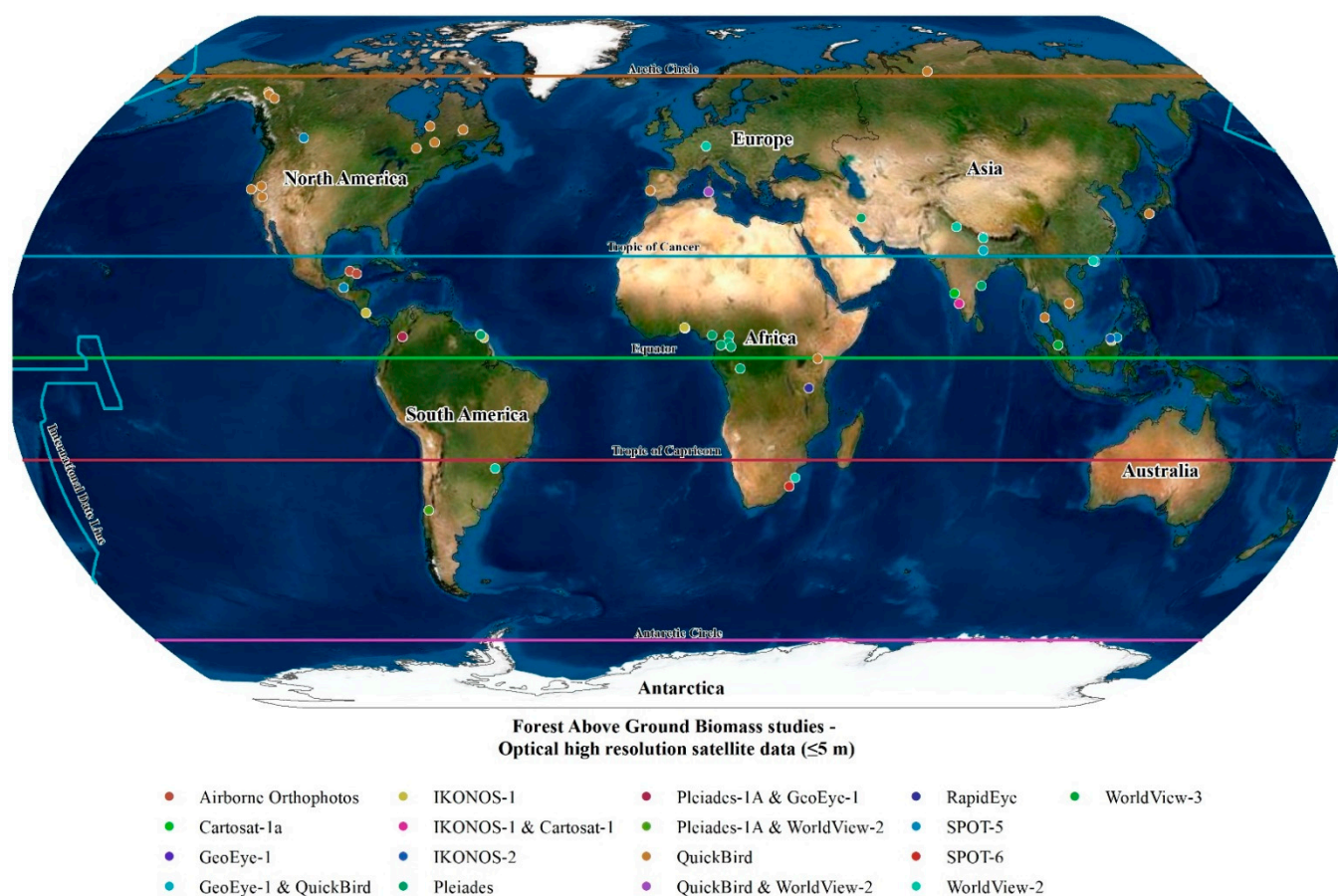


Figure S1. A catalog of 44 peer-reviewed studies published between 2004 to 2019 on forest AGB estimation and mapping through optical high-resolution satellite imagery (≤ 5 m spatial resolution).

Table S1. A catalog of 44 peer-reviewed studies published between 2004 to 2019 on forest AGB estimation and mapping through optical high-resolution satellite imagery (≤ 5 m spatial resolution).

No.	Reference	Continent	Country	Latitude	Longitude	Altitude (m)	The Study Area (ha)	Forest Type	High-Resolution Satellite Data	Other Satellite Data
1	[10]	North America	Costa Rica	10.431	−84.004	35–150	600	Tropical wet evergreen	IKONOS	–
2	[51]	Africa	Benin	6.883 (Site 1) 7.083 (Site 2)	1.683 (Site 1) 1.667 (Site 2)	–	13,500	West African oil palm	IKONOS	–
3	[39]	North America	USA	37.128	−119.29	853–2743	60,000	Mixed coniferous	QuickBird	LiDAR, Landsat ETM+, SAR/inSAR
4	[24]	Africa	Kenya	−0.15	37.3	1200–3400	313,256	Afromontane broadleaf	QuickBird	Landsat ETM+
5	[34]	North America	Canada	49.917 (Site 1)	−74.367 (Site 1)		14,700	Mixed coniferous	QuickBird	–

				53.794 (Site 2)	−77.618 (Site 2)		9300			
				52.908 (Site 3)	−66.869 (Site 3)		10,700			
6	[25]	Africa	French Guiana	4.750 (Site 1)	−52.083 (Site 1)	–	3600 (Site 1)	Mangrove	IKONOS	–
				5.433 (Site 2)	−53.033 (Site 2)		4400 (Site 2)			
7	[35]	North America	Canada	48.5	−79.367	227–348	11,000	Mixed coniferous	IKONOS	LiDAR
8	[47]	Asia	Siberia	67.8	86.717	11	45	Deciduous	QuickBird	ASTER
9	[19]	Asia	Japan	33.266	133.016	–	3300	Coniferous	QuickBird	–
10	[48]	North America	Mexico	16.264	−90.657	–	2000 (Site 1) 2500 (Site 2)	Tropical rainforest	SPOT-5	–
11	[20]	North America	USA	38.890 (Site 1)	−123.320 (Site 1)	–	5900 (Site 1) 5800 (Site 2)	Conifer and hardwood forest	QuickBird	–
12	[21]	North America	Canada	62.294551 (Site 1)	−136.310514 (Site 1)	–	625 (Site 1) 2400 (Site 2) 625 (Site 3) 1375 (Site 4)	Mixed	QuickBird	Landsat ETM+
				61.854901 (Site 2)	−135.672753 (Site 2)					
				61.625741 (Site 3)	−135.379302 (Site 3)					
				60.758427 (Site 4)	−132.745319 (Site 4)					
13	[11]	North America	Canada	51.02	−115.07	1400–2100	18,000	Conifer and deciduous	SPOT-5	–
14	[26]	Asia	Hong Kong	22.331	114.129	–	–	Mixed	SPOT-5	–
15	[52]	North America	Canada	48.5	−79.367	–	16,330	Mixed	QuickBird	–
16	[45]	Africa	South Africa	−27.567	32.35	–	7000	Mangrove	WorldView-2	–
17	[27]	Asia	India	12.538	75.663	200–1000	3000	Wet Evergreen	IKONOS	
18	[53]	Asia	Thailand	9.367	98.4	–	151	Mangrove	GeoEye-1	ASTER
19	[28]	Africa	Congo	−2.485	16.502	300–500	40,000	Mixed	GeoEye-1 and QuickBird	–
20	[12]	Asia	Thailand	9.384	98.416	–	–	Mangrove	QuickBird	–
21	[7]	Asia	Nepal	27.952	84.624	600–1100	5827	Mixed	GeoEye-1	–
22	[13]	Asia	Nepal	27.669	84.624	245–1944	977	Tropical broadleaved	GeoEye-1	–
23	[14]	Asia	Indonesia	4	116	1000–1400	–	Mixed	IKONOS	–
24	[29]	Asia	Malaysia	4.75	117.5	–	7200	Mixed	SPOT-5	–
25	[36]	Europe	Portugal	38.659	−8.121	200	8000	Evergreen oak forests	QuickBird	–
26	[17]	Asia	Nepal	27.669	84.624	245–1944	977	Tropical broadleaved	WorldView-2	LiDAR
27	[55]	Europe	Germany	49.006	8.403	109–114	900	Mixed	Pleiades-1A and	

									WorldView-2	
28	[54]	Europe	Germany	49.006	8.403	109–114	900	Mixed	WorldView-2	EO1-hyperion and Tandem-X
29	[46]	Asia	China	22.42	113.637	–	700	Mangrove	WorldView-2	
30	[43]	South America	Colombia	4.891	–73.942	2800		Mixed	Pleiades-1A and GeoEye-1	
31	[30]		Congo	–2.454267	16.483275	–	28	Tropical forests	Pleiades	–
				5.189338 (Site 1)	13.52147 (Site 1)	–	15			
				5.274167 (Site 2)	9.066293 (Site 2)	–	50			
				3.100774 (Site 3)	13.598995 (Site 3)	–	10			
				3.163553 (Site 4)	13.630282 (Site 4)	–	8			
				–0.750042 (Site 5)	10.58335 (Site 5)	–	12			
				3.556298 (Site 6)	13.414816 (Site 6)	–	11			
				3.576823 (Site 7)	13.396691 (Site 7)	–	12			
				2.624149 (Site 8)	14.026847 (Site 8)	–	6			
				2.941681 (Site 9)	11.394794 (Site 9)	–	5			
				16.749835 (Site 1)	82.189234 (Site 1)	–	15			
				14.943495 (Site 2)	74.694572 (Site 2)	–	22			
				5.274348	–52.925654	–	85			
32	[56]	Asia	India	30.2	77.8	–	–	Tropical moist deciduous forest	WorldView-2	LiDAR (ICESat/GLAS)
33	[16]	Asia	Malaysia	4.451243	115.725106	1150–1500	7036	Tropical rainforest	IKONOS-2	SRTM DEM, LiDAR
34	[31]	Asia	India	12.5375	75.66277778	200–1000	3000	Wet Evergreen forest	IKONOS, Cartosat-1	LiDAR
35	[15]	Europe	Portugal	38.28222222	8.755277778	65	1033	Maritime pine pure stands	QuickBird, WorldView-2	–
36	[32]	Asia	India	14.96225222	74.70614444	457	150,000	Tropical forests	Cartosat-1a	–
37	[18]	Asia	Malaysia	3.006719444	101.6403444	15–233	1248	Tropical forests	WorldView-3	LiDAR
38	[33]	Africa	South Africa	–29.643056	30.976389	200–325	52,060	Tropical dry forest	SPOT-6	–
39	[37]	Asia	Nepal	24.85	84	113–1826	8000	Subtropical forest	GeoEye, QuickBird	Landsat 8 OLI

40	[49]	Asia	Cambodia	12.6821	105.373055	-	48,200	Dry evergreen forest	QuickBird	Airborne LiDAR, digital aerial photographs
41	[44]	South America	Brazil	-25.45	-50.583	893	48	Araucaria forest	WorldView-2	-
42	[50]	North America	Mexico	20.08335 (Site 1) 19.48335 (Site 2)	-89.55 (Site 1) -87.56665 (Site 2)	10 (Site 1) 30 (Site 2)	1800 (Site 1) 47,223 (Site 2)	Tropical dry forest	Airborne Orthophoto s (Vexcel UltraCam LP digital camera)	LiDAR
43	[38]	Asia	Iran	32.25680556	51.42	1960	1500	Mixed	Pleiades	-
44	[23]	Africa	Tanzania	-7	35	-	94,509,000	Mixed	RapidEye	-

Table S2. A list of keywords/terms used in searching for the literature.

Sr. No.	Keywords/Terms
1	AGB
2	Remote sensing
3	Optical data
4	High-resolution
5	Satellite imagery
6	RapidEye
7	SPOT
8	QuickBird
9	IKONOS
10	WorldView
11	GeoEye
12	Biomass estimation
13	Very-high-spatial-resolution
14	AGB quantification
15	Tropical forest biomass
16	Pleiades
17	Cartosat
18	Airborne imagery
19	Forest AGB
20	Tropical forest mapping

Table S3. A database of methodology, accuracy, and average AGB values published in 44 peer-reviewed articles (2004–2019) for forest AGB estimation and mapping using high-resolution satellite imagery.

No.	Reference	Model Applied	Parameters	Number of Samples for Model Formation	Equation	Model Coefficient Value (R^2)	Number of Samples for Model Validation	Validation Coefficient Value (R^2)	Estimated Biomass (kg/ha or ton/ha or Mg/ha)
1	[10]	Linear	Plot basal area = (R^2 = 0.779) and aboveground biomass from stem (EAGB) = (R^2 = 0.786)	18	$Y = 77.6 - 9.7X$	0.63	18	0.786	–

2		Non-linear (Multiple and Exponential)	Ikonos NDVI43 Dry biomass = ($R^2 = 0.63$) Ikonos band 3 dry biomass = ($R^2 = 0.65$)	208	–	Dry biomass = ($R^2 = 0.63$) ($R^2 = 0.65$) Oil palm biomass = ($R^2 = 0.50$) Wet biomass = ($R^2 = 0.72$)	77	0.64 and 0.72	29.5 and 29.88 ton/ha
3	[51]	Non-linear (Multiple and Exponential)	Standard deviation canopy height ($R^2 = 0.64$, RMSE = 3.2) Biomass ($R^2 = 0.83$, RMSE = 66.6 mg/ha)	120	–	0.77	–	0.83	–
4		Linear	For tea, the combination of NIR with homogeneity, entropy and second-moment textures gave the best and similar results ($R^2 = 0.684$). For young pine trees, correlation texture gave the overall best results ($R^2 = 0.741$), and for older pine trees, contrast texture gave the best results ($R^2 = 0.753$) as independent variables	–	–	0.684	–	–	6.502 kg for tea, 7.505 kg for young pine trees (3.5 years old) and 9.779 kg for older pine trees (6 years old)
5		Linear	–	108	–	0.85 to 0.87	32	0.84	163.5 t/ha
6	[39]	Non-linear (multiple and exponential)	We estimated biomass from multiple linear regression models using the three textural indices (scores of the three main PCA axes) as independent variables. Results were compared according to the window size for both PA and NIR data. The best results were obtained from the predictions of AGB values from PA data, with R^2 above 0.87	–	–	0.79	–	0.87	–
7		Linear	–	57	–	0.79	25	–	–
8	[24]	Linear	k-NN	7	–	–	–	–	–

9	Non-linear (multiple and exponential)	The coefficients of determination of the non-linear regression analysis to investigate the relationship between the estimates of parameters a^* and b^* of the allometric model and stand variables such as stand age, stand density, mean stand DBH, mean stand tree height, and relative spacing, simultaneously, were 0.84 and 0.87 for <i>C. japonica</i> and <i>C. obtusa</i> , respectively	26	–	0.58–0.95 0.66–0.94	26	0.64	–
10	Linear (multiple)	The R^2 of the final models was 0.58 for basal area, 0.70 for canopy height, 0.73 for bole volume, and 0.71 for biomass	94	–	0.737	87	0.71	59.3 ton/ha
[34]		Validation of QuickBird crown diameters against field measurements of the same trees showed a significant correlation ($R = 0.82$, $p < 0.05$).						
11	Non-linear (Multiple)	Comparison of stand-level LiDAR height metrics with field-derived Lorey's mean height showed a significant correlation (Garcia-Mailliard $r = 0.94$, $p < 0.0001$; North Yuba $R = 0.89$, $p < 0.0001$).	(1) 38 (2) 40	–	–	–	–	82 ± 0.7 Mg/ha in Garcia-Mailliard and 140 ± 0.9 Mg/ha in North Yuba
12	Non-linear (machine learning)	Regression tree	175	–	–	30	–	–
13	Linear	Regression parameters for crown surface area vs calculated individual tree biomass for lodgepole pine and	36	–	–	36	–	For conifer plots: 30 ton/ha (MFM: 23.0 ton/ha; SMA: 27.9 ton/ha; NDVI: 29.7 ton/ha). The average difference for deciduous

		trembling aspen with coefficient values of $R^2 = 0.63$ and $R^2 = 0.52$, respectively						plots using MFM was 43.8 ton/ha, more than both NDVI (41.7 ton/ha) and SMA (39.3 ton/ha)
14	Linear (multiple)	These were the ratio of the texture parameters of AVNIR-2 ($R^2 = 0.899$ and RMSE = 32.04), the ratio of the texture parameters of SPOT-5 ($R^2 = 0.916$ and RMSE = 29.09), and the ratio of the texture parameters of both sensors together ($R^2 = 0.939$ and RMSE = 24.77)	50	–	0.93	50	0.911	500 ton/ha
15	[25] Non-linear (machine learning)	–	96	$y = 0.0061 \cdot d1.30$	0.978	42	0.843 and 0.816	–
16	Non-linear (machine learning)	The Random Forest regression produced the highest R^2 (0.76), and the lowest root mean square error of prediction (RMSEP) (0.441 kg/m ²) using the three NDVIs compared with the top NDVIs, which produced a R^2 0.63 and RMSEP of 0.505.1 kg/m ² , and the standard NDVI, which yielded an R^2 of 0.31 and a RMSEP of 0.858.1 kg/m ²	82	–	–	25	0.76	3.4365 kg/m ²
17	Linear (multiple)	Stand basal area (BA) and AGB estimates were also closely related to canopy texture indices, and these relationships remained reasonably stable regardless of whether all trees were considered (R^2 ¼ 0.74 and 0.78 for both parameters	15	–	–	–	0.75	–

with GE and IKONOS, respectively) or only the most significant trees (R^2 ¼0.72 and 0.74–0.75 for both parameters with GE and IKONOS, respectively)								
[35]								
18	Non-linear (machine learning)	–	45	AGB = 0.16*[Elevation] + 0.27*[Band 1] – 0.11*[Band 2] + 0.41*[Band 4] – 0.03	–	45	0.66	345 ± 72.5 Mg ha ^{−1}
19	Linear (multiple)	–	26	y = ax + b	–	26	0.85	26 Mg/ha to 460 Mg/ha
[47]								
20	Linear	–	23	y = pxq where x is the independent variable, y is the dependent Variable, and p and q are regression parameters.	0.65	23	0.72	–
21	Linear	The models were validated using a coefficient of determination (linear regression) between calculated stocks through the CPA and DBH relationship and predicted carbon stocks	65	For <i>Shorea robusta</i> = (y = 9.9773x – 88.303) For others = (y = 12.523x – 115.91)	<i>Shorea robusta</i> = 0.65 others = 0.62	20	<i>Shorea robusta</i> = 0.60 others = 0.82	–
[19]								
22	Linear	Development of the relationship between crown projection area (CPA), height, and AGB resulted in accuracies of R^2 ranging from 0.62 to 0.81 and RMSE ranging from 10 to 25% for <i>Shorea robusta</i> and other species, respectively.	109	–	–	91	Community forest (<i>Shorea robusta</i>) = 0.81 Community forest (other species) = 0.62 Government forest (<i>Shorea robusta</i>)	244 and 140 ton C/ha for community and government forests respectively

									= 0.69 Govern ment forest (other species) = 0.73
23	Linear	The field-measured aboveground biomass (AGB_f) was highly correlated with DBH, with R coefficients of 0.85. However, DBH had the highest correlation with CA_I ($R = 0.82$), followed by CD_I ($R = 0.80$) and CP_I ($R = 0.77$). In contrast, relatively low correlations (R coefficient ranges between 0.54 and 0.57) were found between field-measured Ht_f and the satellite-based crown variables.	50	$y = 0.7403x$	0.7197	50	0.7197	50 and 12,000 ton/ha	
24	Linear (multiple)	Regression analysis was carried out for all land-use types, and the FOTO-derived and field AGB values were strongly correlated ($R^2 = 0.9795$, $p = 0.000352$)	196	All land use types (a) = $y = 1.1677x$; Heavily logged forest (b) = $y = 0.7809x$; Old growth forest (c) = $y = 1.125x$; Lightly logged (d) = $y = 0.945x$	(a) = 0.97 (b) = 0.95 (c) = 0.85 (d) = 0.96	–	0.9795	FOTO-derived biomass values indicated that twice-logged forest or LF had an AGB of 120–155 Mg/ha, while oil palm plantations had the lowest FOTO-derived AGB values, 0–80 Mg/ha; the lightly logged forests or the VJR showed very high values for FOTO-derived AGB (180–270 Mg/ha). Small patches of unlogged forest tracts had the highest FOTO-derived AGB values, ranging from 270 to 372 Mg/ha.	

25	Linear	Crown horizontal projection vs aboveground biomass per plot with inventory data ($R^2 = 0.965$)	17	–	Model 1 = 0.900 Model 2 = 0.999	17	0.965	23.2 ton/ha
26	Linear	For this research, a multi-resolution segmentation technique was applied to segment tree crown onto fused LiDAR and WorldView-2 data.	72	<i>S. robusta</i> : $-0.877 + 0.597\text{CPA} + 1.873\text{CHM}$ <i>S. wallichii</i> : $-0.144 + 1.124\text{CPA} + 0.883\text{CHM}$ <i>L. parviflor</i> : $0.205 + 0.370\text{CPA} + 1.494\text{CHM}$ <i>T. tomentosa</i> : $-0.126 + 0.45\text{CPA} + 1.848\text{CHM}$ Others: $0.044 + 0.616\text{CPA} + 1.396\text{CHM}$	0.66 0.75 0.60 0.82 0.64		0.94 0.84 0.78 0.76 0.78	216.38 MgC/ha
27	Non-linear (machine learning)	[20] Random Forest algorithm applied using solely spectral (S), textural (T), or photogrammetric (P) predictors as well as combinations of them, i.e., S+T, S+P, T+P, and S+T+P.	(1) 98 (2) 101	–	–	–		
28	Non-linear (machine learning)	Four semi- or non-parametric regression models in terms of their biomass estimation accuracy: Random Forest, generalized additive models and two boosted algorithms, generalized boosted regression models and the boosted version of the GAM.	303	–	Best results Random Forest: 0.73			29.4 ton/ha
29	Non-linear (machine learning)	A backpropagation artificial neural network (BP ANN) using B5 (red band), B7 (near-infrared-1 band), and B8 (near-infrared-2 band) of	91	–	–	–	–	Mixed species: 72.26 ton/ha Dummy species: 40.15 ton/ha <i>K. candel</i> : 52.38 ton/ha <i>S. apetala</i> : 24.32 ton/ha

		the Worldview-2 images were used to calculate six vegetation indices, including the normalized difference vegetation index (NDVI), the simple ratio index (SRI), and the difference vegetation index (DVI)						
	[21]	Normalized difference vegetation index (NDVI)						
30	Linear	Vegetation index number (VIN) Ratio vegetation index (RVI) Normalized difference greenness index (NDGI) Transformed vegetation index (TVI)	8	Best model $\log \text{AGB} = -3.208 \cdot \text{RVI} + 2.185$	0.582	–	–	–
31	Linear (multiple)	We investigated these simulated images' respective merits of the FOTO method and the lacunarity analysis in predicting AGB both locally (within sites) and globally (across sites). Combined FL model (combining FOTO and lacunarity)	279	–	Best result ($R^2_v = 0.69$)	230	$R^2 = 0.47$	It is noteworthy that site-level MSDs seemed to decrease with the range of biomass encompassed across plots in a site: while plots in Yellapur (MSD = 10.3%) and Paracou (MSD = –18.1%) were restricted to low and high biomass levels, respectively; in Uppangala (MSD = –5.3%) plots have been sampled along a biomass gradient spanning from ~150 up to > 600 Mg ha^{-1} . A practical application of the method to a mosaic of forest types in the Congo basin showed that

								forest AGB inferences could be made with reasonable precision (i.e., ≤25% of error) up to 600 Mg ha ⁻¹ , without saturation. Average AGB over 49 field plots of 359 ± 98 Mg ha ⁻¹
32	Non-linear (machine learning)	Estimation of aboveground biomass (AGB) at ICESat/GLAS footprint level was done by integrating data from multiple sensors using two regression algorithms, viz. Random Forest (RF) and support vector machine (SVM). Multiple linear regression (MLR) was also utilized to estimate AGB when the number of variables was reduced using machine learning regression.	40	Biomass = 0.343 * wdistance + 0.37 * wextent + 0.008 * Correlation2 - 0.0083 * NIR2max - 6.5 * IRGVI2max - SVM regression 0.137 * H75 + 47.125 where wdistance = top tree height wextent = LiDAR spectral parameter Correlation2 = texture parameters NIR2max = Satellite image spectral parameter IRGVI2max = Satellite image spectral parameter H75 = Satellite image spectral parameter		–	–	It was found that the SVM regression algorithm explained 88.7% of the variation in AGB with an RMSE of 13.6 Mg ha ⁻¹ on the combined datasets, while the RF regression algorithm explained 83.5% of the variation in AGB with an RMSE of 20.57 Mg ha ⁻¹ .
33	Linear	Normalized difference vegetation index (NDVI) Pearson's correlation was used to test which of these variables was	50	Intact forest: AGBT (intact forest) = exp(2.62 · ln DBH-2.30) Degraded forest: AGBT (degraded	Intact forest regression = 0.89 degraded forest regression = 0.87	25	Intact forest regression on: R ² = 0.812 Degraded forest regression	Average of 1058 kg for intact forest and 147 kg for degraded forest

		most closely related to field-derived AGB. Least square regression was used for generating a statistical model		forest)=0.0829 ·DBH2.43		on = 0.7142		
34	Linear (multiple)	Fourier transform based textural ordination (FOTO)	15	–	IKONOS $R^2 = 0.82$ Carto-A $R^2 = 0.76$ Carto-F $R^2 = 0.76$	–	–	The estimated AGB values from the 15 large (1 ha) plots covered a significant range of biomass varying from a minimum of 124 t ha ⁻¹ to a maximum of 684 t ha ⁻¹ , with an average of 435 t ha ⁻¹ . RMSEs computed for predicted and field measured biomass using IKONOS and Carto-A imagery were 67.03 and 77.32 t ha ⁻¹
[11]				$W = ww + wbr + wl$ $wl = 0.09980 * d ^ {1.39252} * (h/d)^{0.71962}$ $wbr = 0.0308 * d^{2.75761}*(h/d)^{-0.39381}$ $ww = 0.0146*d^{1.94}687*h^{1.10657}$ 7 <p>where d is the diameter at breast height, h is the total height, W is the total above ground biomass, ww is the biomass of wood, wbr is the biomass of branches, wl is the biomass of leaves.</p> $W = b*CHP$ <p>where b is the regression</p>				
35	Linear	Normalized difference vegetation index (NDVI)	57		$R^2 = 0.719$	–	–	The aboveground biomass estimated with M5 was 32.3 Mg ha ⁻¹ in 2004, 16.3 Mg ha ⁻¹ in 2007, and 10.8 Mg ha ⁻¹ in 2011

				coefficient, W is the aboveground biomass, CHP is the crown horizontal projection,				
36	Linear (multiple)	Fourier transform based textural ordination (FOTO)	21	AGBtree = 0.0673 $(q \cdot DBH^2 \cdot H)$ $\wedge 0.0976$	$R^2 = 0.82$	-	$R^2 = 0.76$	The predicted mean AGB values for the wet zone plots ranged between 141 Mg ha^{-1} and 486 Mg ha^{-1} A separate texture–AGB model was fitted for dry zone ground control plots, which predicted low biomass values ranging between 159 Mg ha^{-1} to 228 Mg ha^{-1}
37	[26] Linear (multiple)	Ordinary least squares (OLS)	166 (no. of trees out of 32 two-ha plots)	AGBest = 0.0673 $(q \cdot DBH^2 \cdot H)$ $\wedge 0.0976$	$R^2 = 0.952$ (best model)	79 (no. of trees out of 32, two-ha plots)	$R^2 =$ 0.914 (best Model)	655–12,300 kg/trees (best model)
38	Linear (multiple)	The relationship between natural forests aboveground biomass and image texture variables was modeled using a Random Forest (RF) algorithm and multiple linear regression (MLR). Raw band textures, two-band textures, and three-band texture using multiple linear regression and Random Forest regression	63 plots	AGB = $0.112 \times$ $(qD^2H)0.916$, where AGB is total aboveground biomass, q is wood density, D is the diameter at ground level, and H is total tree height.	Multivariate analysis results for the three image processing techniques showed that single-texture bands produced the lowest overall accuracy ($R^2 =$ 0.64 and $RMSE$ $= 94.13 \text{ kg m}^{-2}$) followed by some improvements using the two- band texture combination ($R^2 = 0.85$ and $RMSE = 60.65$ kg m^{-2}). However, the highest overall accuracy was obtained using	27	Three- band texture models produce d the highest overall predicte d perform ance with an R^2 of 0.88 and 0.77 compar ed with both the two- band texture ratios ($R^2 =$ 0.85 and 0.67) and the	268.79 kg/m^{-2}

					the three-band texture combination ($R^2 = 0.88$ and RMSE = 54.54 kg m ⁻²).		raw texture bands ($R^2 = 0.64$ and 0.53)	
[52]		Tree canopy cover (TCC) vs. forest aboveground biomass (FAGB) model. A multivariate adaptive regression splines (MARS) machine learning algorithm was used to develop a model from the relationship between different predictor parameters from Landsat 8 bands and its vegetation indices with the FAGB of GEVHR virtual sample plots.						
39	Linear		30 plots	$y = 1.0865x - 62.078$	(R^2) of 0.76	20	(R^2) = 0.83	The average forest aboveground carbon (FAGC) estimated was 260 tons ha ⁻¹ , while in the field, it was 249 tons ha ⁻¹
40	Linear (multiple)	Multiple regression analysis Digital canopy model (DCM)	57 plots	AGB = exp (2.134 + 2.530 ln (DBH)) AGBF = 0 + 1 hmax + 2 hmin + 3 hmean for LiDAR AGBL = 0 + $\sum_{k=1}^5 (k_{mk} + k_{sk})$ for satellite data	$R^2 = 0.90$ for LiDAR $R^2 = 0.73$ for satellite data	–	–	RMSE = 38.7 Mg/ha from LiDAR RMSE = 42.8 Mg/ha from aatellite data
[45]								
41	Linear	Simple reason (SR) NDVI (normalized difference vegetation index) SAVI (soil-adjusted vegetation index)	29	Bio = $\beta_0 + \beta_1 \cdot \text{DBH} + 14.4 \cdot 0.86 - 2901.85 \cdot 96.3$ Bio = $\beta_1 \cdot \text{NDVI}_2 + 37.8 \cdot 0.87 - 23168.7$ Bio = $\beta_1 \cdot \text{B1} + 38.8 \cdot 0.87 - 51.8$ Bio = $\beta_1 \cdot (\text{NDVI}) + \beta_2 \cdot (\text{SR}) + \beta_3 \cdot (\text{SAVI})$	0.87	–	–	–
42	Linear (multiple)	Normalized difference vegetation index	48	–	Site 1 (LiDAR $R^2 = 0.82$ and Orthophoto R^2	.	Site 1 (LiDAR $R^2 = 0.62$	Site 1 (LiDAR RMSE = 35.5 mg ha ⁻¹ and

		(NDVI) Enhanced vegetation index (EVI)			= 0.70) Site 2 (LiDAR $R^2 = 0.88$ and Orthophoto R^2 = 0.91) Combined = 0.85		and Orthoph oto $R^2 =$ 0.52) Site 2 (LiDAR $R^2 = 0.85$ and Orthoph oto $R^2 =$ 0.86) Combin ed = 0.69	Orthophoto RMSE= 42.6 mg ha ⁻¹) Site 2 (LiDAR RMSE = 14.4 mg ha ⁻¹ and Orthophoto RMSE= 13.6 mg ha ⁻¹) Combined = 33.0 mg ha ⁻¹
	[27]				Bt = Bs + Bsb + Bb + Bt + Bf, where Bt is the total aboveground biomass, Bs is the stem, Bsb is the stem bark, Bb is the branch, and Bt is the twig, Bf is the foliage biomass. All parts of trees were separated, followed by in situ measurement of each part's total fresh weight.			In this study, the highest amount of carbon sequestration was estimated for <i>P.</i> <i>eldarica</i> (4462.18 t ha ⁻¹), followed by <i>C. arizonica</i> (2103.37 t ha ⁻¹) plantations, whereas the lowest amount was estimated for <i>M. alba</i> (1009.09 t ha ⁻¹) and <i>R.</i> <i>pseudoacacia</i> (365.38 t ha ⁻¹) plantations.
43	Linear	DBH, height, crown diameter, and stem length	48		Total biomass $R^2 = 0.90$ (RMSE = 24.92 t ha ⁻¹) Dry biomass R^2 = 0.91 (RMSE = 12.74 t ha ⁻¹)	–	–	
44	Linear	Mean bands 1 to 5 Standard deviation bands 1 to 5 The ratio of mean to the standard deviation for all bands Standard deviation. Ratios Red vegetation index Green vegetation index Green red vegetation index Normalized difference vegetation index Enhanced vegetation index	85% for training Random Forests (RF)– 435 plots out of 500	AGB = $D \times \bar{y}$, where D is the total study area and \bar{y} is the average AGB ha ⁻¹ of the sample areas	The best results were found using the Random Forests algorithm ($R^2 =$ 0.69)	15% for training Random Forests (RF)–77 plots out of 500	RF with very high accuraci es (i.e., RMSE~1 5, $R^2 =$ 0.93),	We found an average of 22.1 tons per ha of aboveground biomass (AGB)

Soil-adjusted
vegetation index
Shadow index
Modified transverse
vegetation index
Modified
chlorophyll
absorption
reflectance index
Bare soil index
Shadow to soil ratio
GLCM texture
features
Bare soil
Shadow
